AIP | Applied Physics Letters

The influence of Hausdorff dimension on plasmonic antennas with Pascal's triangle geometry

S. Sederberg and A. Y. Elezzabi

Citation: Applied Physics Letters **98**, 261105 (2011); doi: 10.1063/1.3605570
View online: http://dx.doi.org/10.1063/1.3605570
View Table of Contents: http://scitation.aip.org/content/aip/journal/apl/98/26?ver=pdfcov
Published by the AIP Publishing

The influence of Hausdorff dimension on plasmonic antennas with Pascal's triangle geometry

S. Sederberg[a] and A. Y. Elezzabi
Ultrafast Optics and Nanophotonics Laboratory, Department of Electrical and Computer Engineering, University of Alberta, Edmonton T6G 2V4, Canada

(Received 17 May 2011; accepted 8 June 2011; published online 29 June 2011)

We introduce fractal geometry to the common bowtie antenna and investigate the influence of a key fractal parameter, Hausdorff dimension, on the broadband spectral response of the antenna. Length scaling trends are presented for antennas having various Hausdorff dimensions. We show that antennas with Pascal's triangle geometry accommodate resonances that are red-shifted when compared to a standard bowtie antenna having the same size. Furthermore, increasing the Hausdorff dimension of the antenna blue shifts its resonance. By designing nanoplasmonic antennas with Pascal's triangle geometry, the resonance conditions may be varied while the antenna dimensions are kept constant. © *2011 American Institute of Physics*. [doi:10.1063/1.3605570]

Plasmonic antennas can be used to confine electromagnetic energy to a sub-wavelength scale in all three spatial dimensions.[1–5] In general, these antennas are composed of one or more noble metal nanostructures that support a geometry-dependent plasmon resonance. Driving the antenna at this resonance enhances incident electric fields by two orders of magnitude in the antenna gap and allows access to weak physical effects that would be unobservable with a standard light source.[6,7] Typical antenna geometries consist of rods, spheres or triangles. Interestingly, the broadband spectral response of radio-frequency, microwave, and terahertz antennas has been shown to depend strongly on the antenna geometry.[8,9] As such, the operating frequency of the antenna and other important antenna properties may be controlled by carefully designing its shape. Unlike their microwave antenna counterparts, developments in plasmonic antennas have produced relatively little geometric diversity. When considering antennas for optical and infrared wavelengths, the antenna length shrinks to nanometers or micrometers, making it difficult to investigate anything but the simplest designs, such as a bowtie or dipole antenna. Only recently have fabrication techniques such as electron beam lithography and focused ion beam lithography made it possible to define complex shapes with features on the order of tens of nanometers. An interesting class of antenna geometry that has been investigated in the microwave frequency range is fractal antennas.[10,11]

Recently, the influence of fractal iteration on the operation of Sierpiński triangle antennas resonant in the near- to mid-infrared was investigated, and it was found that increasing the iteration yields red-shifted resonance conditions.[12] These investigations were performed for a fixed Hausdorff dimension (i.e., D = 1.585). However, it is more fundamental to examine the influence of the Hausdorff dimension on the antenna performance. In this paper, we demonstrate that fractal antennas of varying Hausdorff dimensions consistently exhibit red-shifted resonance conditions when compared to a bowtie antenna of the same size and we investigate the relationship between the Hausdorff dimension and the antenna resonance.

Fractals are different from standard geometric shapes such as polygons and arcs because they contain infinite detail and as one magnifies a fractal structure further and further, the new details that appear have the same form as those in the parent structure. In this respect, fractals are said to be self-similar on multiple length scales. A fractal may be represented by a basis shape and an operator that acts iteratively on that shape. One well-known fractal is Sierpiński's triangle, shown in Figs. 1(a)–1(d), whose basis shape is a triangle. Going from the basis shape in Fig. 1(a) to the first iteration shape in Fig. 1(b), three triangles, each one-quarter of the area of the original triangle, are arranged to fill the outline of

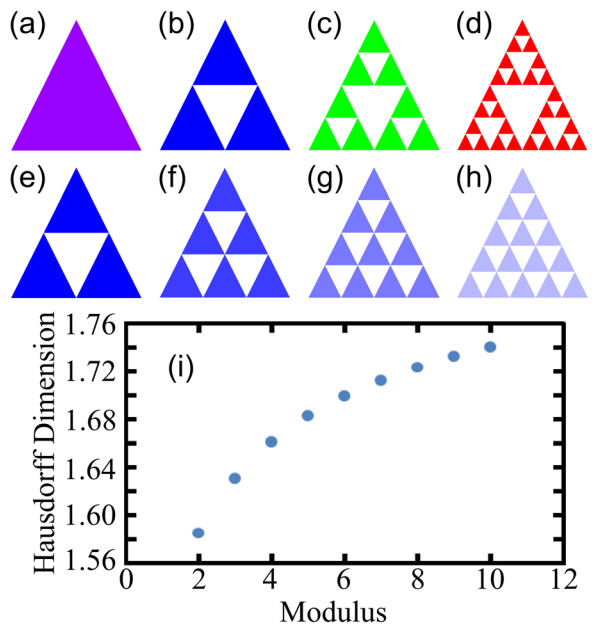

FIG. 1. (Color online) (a) Sierpiński triangle basis shape and (b)-(d) first three iterations of Sierpiński triangle. (e)-(h) Modulus M = 2, 3, 4, and 5 Pascal's triangles, respectively. (i) The relationship between modulus and Hausdorff dimension for a Pascal triangle.

[a]Author to whom correspondence should be addressed. Electronic mail: hiroaki@ee.t.u-tokyo.ac.jp.

the original triangle. In subsequent iterations, this same operation is applied to each triangle that composes the fractal. The common bowtie antenna is shown in Fig. 2(a). Placing two Sierpiński triangles next to one another produces a structure that is similar to the bowtie antenna, but contains fractal features, as shown in Fig. 2(b).

A fundamental parameter of a fractal is the Hausdorff dimension, which describes how the length scale decreases as the iteration increases and how the number of features composing the fractal multiplies as the iteration increases.[13,14] In performing an investigation into the relationship between Hausdorff dimension and antenna performance, it would be ideal to keep the antenna outline constant while modifying only the internal structure of the antenna to vary the Hausdorff dimension. A geometric abstraction of Sierpiński's triangle that satisfies this requirement is a class of triangles known as Pascal's triangles. The first four moduli of Pascal's triangles are shown in Figs. 1(e)–1(h). As the modulus, M, increases, the size of the triangle that makes up the structure decreases and the number of triangles composing the structure increases. The Hausdorff dimension can be related to the modulus by the following formula:

$$D = \frac{\log\left(\sum_{m=1}^{M} m\right)}{\log(M)}.$$

This relationship is plotted in Fig. 1(i). Notably, Sierpiński's triangle is a modulus two (M = 2) Pascal's triangle. Schematic depictions of antenna geometries for the second (M = 2), third (M = 3), and fourth (M = 4) moduli of Pascal's triangle are shown in Figs. 2(b)–2(d).

Although an antenna may support more than one resonance, we only consider the resonance with the greatest amplitude. This occurs at a longer wavelength (typically 1.0 μm $\leq \lambda \leq$ 3.0 μm) than the weaker resonances (typically $\lambda \leq$ 1.0 μm), and therefore, makes the most efficient use of the

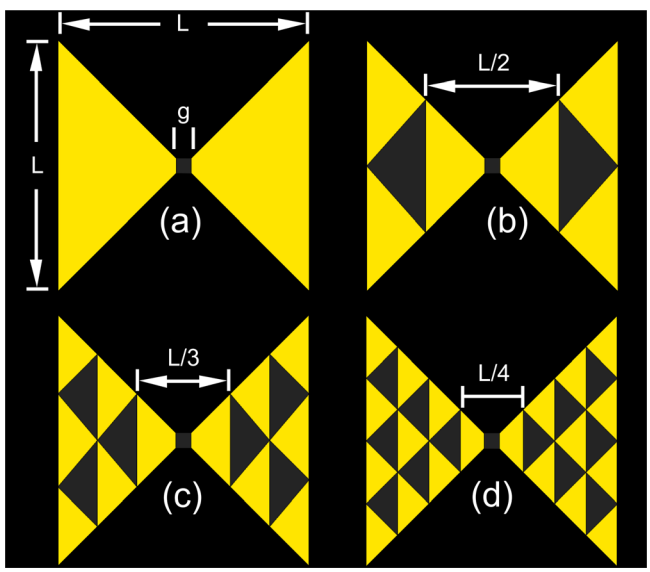

FIG. 2. (Color online) Schematic representation of (a) bowtie antenna and bowtie antennas with Pascal's triangle modulus (b) M = 2, (c) M = 3, and (d) M = 4 geometry.

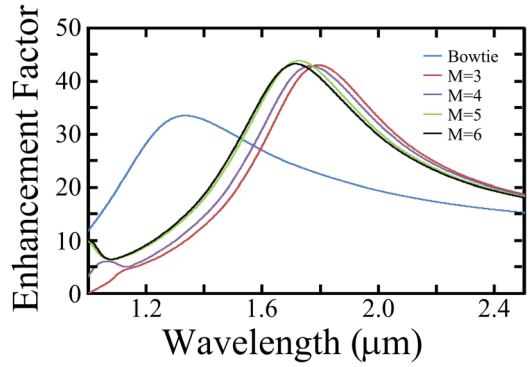

FIG. 3. (Color online) Broadband enhancement factor for a bowtie antenna with L = 475 nm, along with M = {3,4,5,6} antennas with L = 475 nm.

antenna footprint. For example, the primary resonance of an M = 3 antenna with length, L = 475 nm, is at λ = 2.01 μm, as shown in Fig. 3. Increasing the modulus to M = 4, 5, and 6 produces resonances at λ = 1.98 μm, λ = 1.93 μm, and λ = 1.91 μm, respectively, also shown in Fig. 3. A simple bowtie antenna with L = 475 nm is found to resonate at λ = 1.41 μm. Therefore, bowtie antennas with Pascal's triangle geometry produce resonances that are substantially redshifted relative to a standard bowtie antenna. Notably, the observed 50% change in the resonance frequency allows these antennas to operate at longer wavelengths without increasing the size of the antenna. This unique feature allows the antenna to confine light of a longer wavelength to the same nanoscale dimensions as a bowtie antenna.

Logarithmic plots of the near-field intensity distribution of modulus M = 3, 4, and 5 antennas at their resonances are shown in Figs. 4(a) 4(c), and 4(e) respectively. These

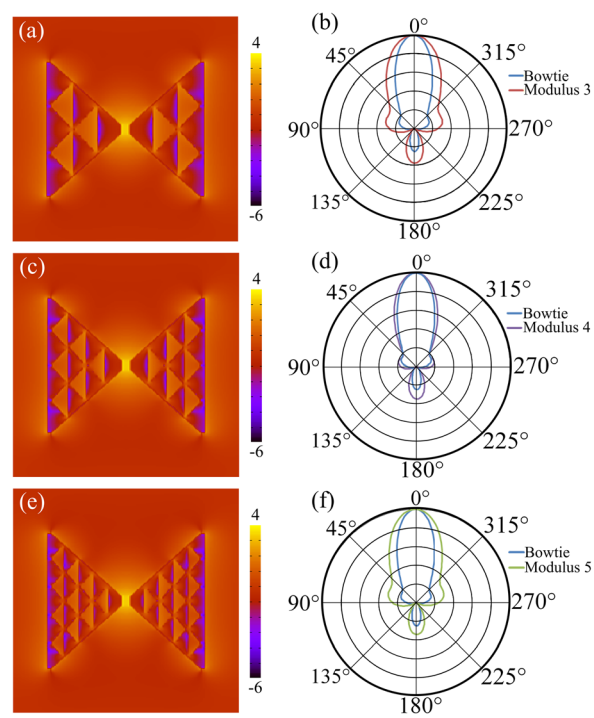

FIG. 4. (Color online) Logarithmic scale intensity distributions for (a) M = 3, (c) M = 4, and (e) M = 5 antennas. Intensity distributions are normalized to the input excitation. Directivity plots for (b) M = 3, (d) M = 4, and (f) M = 5 antennas. Directivity plots of a bowtie antenna are included for reference.

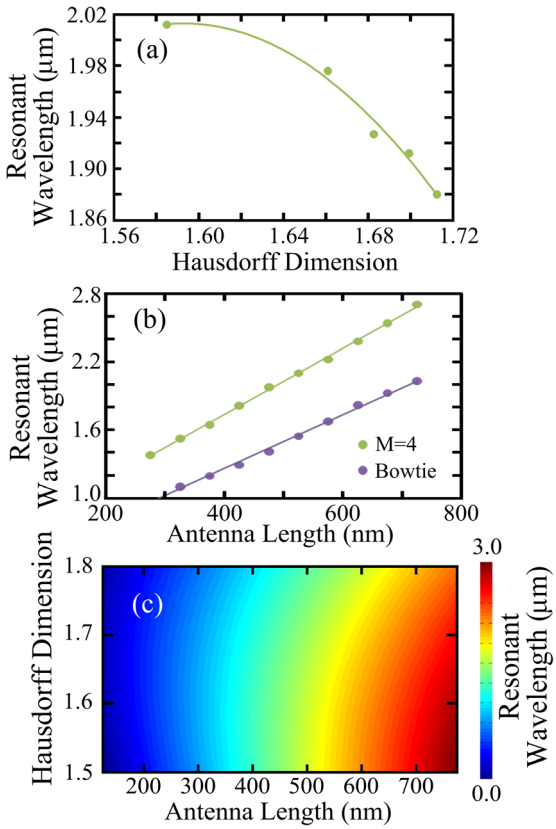

FIG. 5. (Color online) (a) Resonant wavelength versus modulus for $L = 475$ nm (constant). A parabolic trend line is included. (b) Resonant wavelength versus antenna length for $M = 4$ (constant). The trend for a bowtie antenna is shown for comparison. (c) Paraboloid surface-fit to resonant wavelengths of 55 antennas that were simulated.

distributions are normalized to the amplitude of the input excitation. Regardless of the value of M, the incident electromagnetic energy is largely confined to the antenna gap and not to other regions of the antenna. Directivity plots of modulus M = 3, 4, and 5 antennas at their resonances are shown in Figs. 4(b) 4(d), and 4(f), respectively, along with the directivity plot of a bowtie antenna for reference. Introducing fractal geometry to the antenna tends to widen the main lobe, increase the amplitude of the back lobe, and increase the amplitude of the side lobes when compared to a bowtie antenna. For example, modulus {3, 4, 5} antennas have half-power beam widths of {69.8°, 50.5°, 65.2°}, whereas a bowtie antenna has a half-power beam width of 43.4°. Although the directivity of the fractal antennas is inferior to the bowtie antenna, it is evident from the plots that strong directivity is present and that they are functional antennas.

A total of fifty-five antenna structures with moduli in the range $2 \leq M \leq 10$ and lengths in the range $175 \leq L \leq 725$ nm are used to investigate the influence of Hausdorff dimension on the antenna behavior. As a typical example, the resonant wavelength is plotted versus the Hausdorff dimension for a constant antenna length, $L = 475$ nm, and it is observed that as the Hausdorff dimension increases, the resonant wavelength decreases in a manner that is approximately parabolic, as shown in Fig. 5(a). Considering the converse, we plot the resonant wavelength versus the antenna length for a constant modulus, $M = 4$, as shown in Fig. 5(b). In the same manner as a standard bowtie antenna (also shown in Fig. 5(b)), the resonant wavelength scales linearly with the antenna length. A paraboloid of the form $\lambda = c_1L^2 + c_2L + c_3D^2 + c_4D + c_5LD + c_6$ is fit to data from the 55 antennas with $\{c_1,c_2,c_3,c_4,c_5,c_6\} = \{-1.43 \times 10^{-5}, 7.92, -3.53 \times 10^3, 1.22 \times 10^5, -3.03, -1.00 \times 10^5\}$ and $R^2 = 0.994$, where D is the Hausdorff dimension. This surface is shown in Fig. 5(c). Examining this plot, it can be observed that the antenna length is a sensitive parameter for adjusting the resonant wavelength, regardless of the Hausdorff dimension. Interestingly, the Hausdorff dimension can equally be used to achieve fine tuning of the antenna resonance.

Changing the Hausdorff dimension of the Pascal's triangles composing an antenna modifies the internal structure of the antenna while keeping its outline shape constant. A Pascal's triangle can be viewed as a periodic lattice of smaller triangles. Increasing the Hausdorff dimension decreases the lattice period and increases the overall number of smaller triangles in the structure. When excited at resonance, the entire lattice of triangles must become polarized. The smaller triangles require a shorter wavelength for resonant polarization, so the resonance shifts to the blue.

In conclusion, we have investigated the operation of plasmonic bowtie antennas that have been modified to include Pascal's triangle geometry. Length-scaling trends for antennas with various Hausdorff dimensions have been presented, as has the influence of Hausdorff dimension on the antenna resonance conditions. We anticipate that the results from this investigation will contribute to both theoretical and experimental investigations into plasmonic antennas with fractal and other complex geometries.

This work was supported by the Natural Sciences and Engineering Research Council of Canada, Alberta Innovates, and the Canadian Research Chairs program.

[1]P. Mühlschlegel, H.-J. Eisler, O. J. F. Martin, B. Hecht, and D. W. Pohl, Science **308**, 1607 (2005).
[2]M. Schnell, A. Garcia-Etxarri, A. J. Huber, K. Crozier, J. Aizpurua, and R. Hillenbrand, Nature Photon. **3**, 287 (2009).
[3]H. Fischer and O. J. F. Martin, Opt. Express **16**, 9144 (2008).
[4]K. B. Crozier, A. Sundaramurthy, G. S. Kino, and C. F. Quate, J. Appl. Phys. **94**, 4632 (2003).
[5]D. P. Fromm, A. Sundaramurthy, P. J. Schuck, G. Kino, and W. E. Moerner, Nano. Lett. **4**, 957 (2004).
[6]S. Kim, J. Jin, Y.-J. Kim, I.-Y. Park, Y. Kim, and S.-W. Kim, Nature **453**, 757 (2008).
[7]R. Adato, A. A. Yanik, J. J. Amsden, D. L. Kaplan, F. G. Omenetto, M. K. Hong, S. Erramilli, and H. Altug, Proc. Natl. Acad. Sci. U.S.A. **106**, 19227 (2009).
[8]J. D. Kraus, *Antennas* (McGraw-Hill, New York, 1988).
[9]H. Jasik, *Antenna Engineering Handbook* (McGraw-Hill, New York, 1961).
[10]D. H. Werner and S. Ganguly, IEEE Antennas Propag. Mag. **45**, 38 (2003).
[11]C. Gaubert, L. Chusseau, A. Giani, D. Gasquet, F. Garet, F. Aquistapace, L. Duvillaret, J.-L. Coutaz, and W. Knap, Phys. Status Solidi C **1**, 1439 (2004).
[12]S. Sederberg and A. Y. Elezzabi, Opt. Express **19**, 10456 (2011).
[13]B. B. Mandelbrot, *The Fractal Geometry of Nature* (W.H. Freeman, San Francisco, 1982).
[14]K. J. Falconer, Fractal Geometry: *Mathematical Foundations and Applications* (Wiley, Chichester, 2003).